Thermal conductivity of compacted Opalinus Clay at different degrees of saturation

Nuria Sau[1,2*], *Florian* Christ[3], *Enrique* Romero[1,2], and *Arash Alimardani* Lavasan[3]

[1]Centre Internacional de Mètodes Numèrics en Enginyeria CIMNE, Barcelona, Spain
[2]Universitat Politècnica de Catalunya UPC, Barcelona, Spain
[3]Ruhr-Universität Bochum RUB, Bochum, Germany

Abstract. Tunnelling in bedded shale rocks induces damage around the excavation. Consequently, the rock mass in the excavation damaged zone (EDZ) shows different thermo-hydro-mechanical (THM) properties from the intact rock. In turn, the damaged material close to the tunnel wall is affected by seasonal fluctuations in temperature and relative humidity (RH) variations associated with tunnel ventilation, impacting the total suction and the saturation state of the EDZ. The monitoring data at the new Swiss Belchen A2 highway tunnel excavated in Opalinus Clay (OPA) captured these seasonal variations in the total stress acting on the lining associated with this temperature and RH fluctuation. Within this context, assessing the temperature field in the EDZ requires determining the thermal conductivity of the damaged rock at different degrees of saturation. However, obtaining good-quality cores of OPA from the EDZ is not straightforward, and partially desaturating them using controlled RH techniques is time-consuming. Consequently, instead of testing damaged OPA, statically compacted samples of OPA powder at different degrees of saturation have been considered to study the thermal conductivity. In addition, two natural OPA samples (with different bedding orientations) retrieved from the Belchen tunnel have been tested to cross-check the experimental procedure and results, which indicated a consistent increase in thermal conductivity with the degree of saturation.

1 Introduction

Infrastructure tunnels are a significant part of the mobility transition. They are designed for long service life. However, due to swelling phenomena, several structural damages have been observed in road tunnels constructed in anhydrite-rich rocks or clay rocks [1–5]. While mechanised tunnelling, there are stress redistribution and dilation in the vicinity of the tunnel, which results in the formation of a so-called Excavation Damaged Zone (EDZ). Physically damaged and destructured rock mass in the EDZ shows different thermal, hydraulic and mechanical properties. Additionally, the formation of the EDZ potentially triggers volume change phenomena due to the opening of preferential flow paths in relatively dry materials along the tunnel and pore water disequilibrium due to the excavation-induced unloading and ventilation.

Besides solely hydro-mechanical processes, also temperature plays a significant role in the total stresses acting on the tunnel support system. This was observed at the new Belchen A2 highway tunnel tube (STB) in Northern Switzerland, constructed between 2016 and 2020, and excavated in the argillaceous formation Opalinus Clay and the anhydrite-rich rock Gipskeuper. As the old tunnel tubes were consistently exposed to swelling of the surrounding argillaceous and anhydrite formations since its construction in the 1960s resulting in recurring structural damages, the STB was comprehensively equipped with monitoring equipment for short- and long-term measurements. Data [6] clearly show cyclic temperature-driven variations of the radial stress on the tunnel lining induced by seasonal changes. They are around 0.4 MPa for annual temperature changes of 10°C in the Opalinus Clay, the rock mass studied in the present research. Preliminary thermomechanical simulations support the expected impact of thermally-induced expansion and contraction of the Opalinus Clay, but also indicate missing additional influences in the simulations, such as those related to the de- and resaturation of the rock mass around the excavation due to seasonal variations in relative humidity (RH) [6]. Changes in the degree of saturation impact the temperature field distribution around the EDZ of the tunnel lining since water's thermal conductivity is one order of magnitude higher than air. Thereby, characterising the thermal conductivity of the damaged and partially desaturated Opalinus Clay is essential to properly asses the temperature field. However, testing OPA cores from EDZ controlling the degree of desaturation using RH techniques is not straightforward, mainly because obtaining good quality samples at a real construction site requires considerable technical effort and vapour equilibrium is time-consuming. Consequently, instead of testing damaged OPA, statically compacted samples

* Corresponding author: nuria.sau@upc.edu

of OPA powder at different degrees of saturation have been used to study the thermal conductivity. In addition, the thermal conductivity of two natural Opalinus Clay samples on two different orientations (heat flow parallel and perpendicular to bedding planes) was also studied. This additional data allowed for building confidence in the experimental setup and procedures since Opalinus Clay has been widely studied as the selected host rock formation for the deep geological repository of heat-emitting and long-lived radioactive waste in Switzerland (for instance, [7–10]).

2 Experimental program

The sections below present the material tested, a brief description of the testing equipment, and the procedures followed.

2.1 Material tested

Opalinus Clay is a Jurassic-aged marine claystone formation. It is composed of several facies and subfacies types according to the amount of quartz, carbonates and clay minerals. The tested Opalinus Clay was retrieved at the construction site of the new Belchen highway tunnel (Jura Mountains in Northern Switzerland), which connects Basel and Lucern. Drilling cores were extracted under consideration of the bedding plane orientation at a depth of around 300 – 340 m [11]. The mineralogical analyses showed a similar composition to the shaly facies of Opalinus Clay at Mont Terri Underground Research Laboratory (URL) [12]. The average mass percentage of clay minerals is 64.4%, composed of 22.8-31.4% muscovite/illite, 17.0-21.1% kaolinite, 11.1-16.0% illite/smectite and 4.0-6.5% chlorite. The non-clayey fraction mainly comprises quartz (17.8%) and carbonate minerals (11.6%).

Intact natural samples, parallel and orthogonal to the bedding direction, were prepared from two different drilling cores by reducing the diameter with a lathe and subsequently cutting with a diamond band saw to the final height. Opalinus Clay powder was obtained using a jaw crusher and the dry rock of the drilling core from the intact parallel sample. The material was crushed to pass through the sieve with a maximum diameter of 0.25 mm. For producing artificially prepared samples of Opalinus with different initial degrees of saturation, the corresponding amount of additional water was added to the powder, and the mixture was sealed and homogenised for 24 h. Afterwards, the mixture was statically compacted in a press to a defined volume to reach the target dry density of 2.0 Mg/m³, which resulted in a void ratio of 0.338. To ensure homogeneity on samples, the uniaxial static compaction was performed from both the top and bottom sides. The initial parameters of the intact samples are summarised in Table 1, and of the statically compacted samples in Table 2. The total suction Ψ was measured using a chilled mirror dew-point psychrometer (details of this technique in [13]). The high total suction of the saturated or nearly saturated OPA intact samples results from the large matric suction induced on water-undrained unloading upon retrieval.

Table 1. Properties and the initial state of the two intact OPA samples.

	OPA-bed ⊥	**OPA-bed ∥**
Water content, w (%)	4.53	3.73
Void ratio, e (-)	0.12	0.12
Degree of saturation, Sr (-)	0.98	0.83
Total suction, Ψ (MPa)	~ 60	
Density of solids, ρ_s (Mg/m^3)	2.68	
Dry density, ρ_d (Mg/m^3)	2.4	2.4

Table 2. Initial state of the statically compacted OPA samples.

ID Samples	w **(%)**	Ψ **(MPa)**	Sr **(-)**
Comp-OPA-1	3.50	54	0.18
Comp-OPA-2	6.15	13	0.49
Comp-OPA-3	8.24	9.0	0.65
Comp-OPA-4	10.61	3.5	0.84
Comp-OPA-5	11.91	1.5	0.94

2.2 Testing setup and protocols followed

Tests were carried out in an experimental setup developed within the context of the Project 'Thermal aspects and their coupled HM effects on Ypresian clays and Boom Clay', a collaboration agreement between ONDRAF/NIRAS (Belgium) and CIMNE (Spain). It was designed to determine the thermal conductivity at high stresses using a rigid PEEK^{TM} cell [14] to reduce radial thermal losses and a lever mechanism to apply vertical stresses. Before and during the thermal tests, high vertical stresses were required to mimic in situ stress conditions (4.5 MPa) at the Belchen tunnel.

Thereby, thermal resistivity interferences resulting from stress relief during undrained retrieval of intact samples (opening of bedding planes) or the one occurring on undrained unloading after static compaction (poor contact between the heating cap and sample) were avoided. The cell was designed to apply a

controlled high temperature at the top of a cylindrical specimen (38 mm in diameter and 40 mm high). Seven thermocouples continuously monitored the temperature at three internal points of the soil sample and at the top and bottom heat flux sensors. Figure 1 shows a cross-section of the cell. The heat flux sensors made of reference materials (a polycarbonate disc with λ_{poly}=0.20 $Wm^{-1}K^{-1}$ and thickness t_{disc}=1 mm placed between two highly conductive aluminium discs with 209 $Wm^{-1}K^{-1}$) allowed determining the input q_{in} and output q_{out} heat fluxes using Fourier's law and assuming negligible thermal gradient in the aluminium discs:

$$q_{in} = -\lambda_{poly}\, \Delta T_{top} / t_{disc} \text{ and } q_{out} = -\lambda_{poly}\, \Delta T_{bot} / t_{disc} \quad (1)$$

ΔT_{top} and ΔT_{bot} are the temperature difference between aluminium discs on both top (thermocouples T_1 and T_2) and bottom (thermocouples T_6 and T_7) heat flux sensors.

The water content loss was prevented by covering the soil sample with a neoprene membrane and keeping the testing times as short as possible. Usually, tests lasted 5 hours to reach steady-state conditions.

The cell made of PEEK™ provided radial stiffness and thermal insulation, as previously indicated. In addition, an additional external layer of heat-insulating foam (polyisocyanurate foam) was placed to reinforce thermal insulation.

The thermal conductivity tests were performed at an average maximum temperature close to 45°C and with a change in temperature across the sample around 15°C.

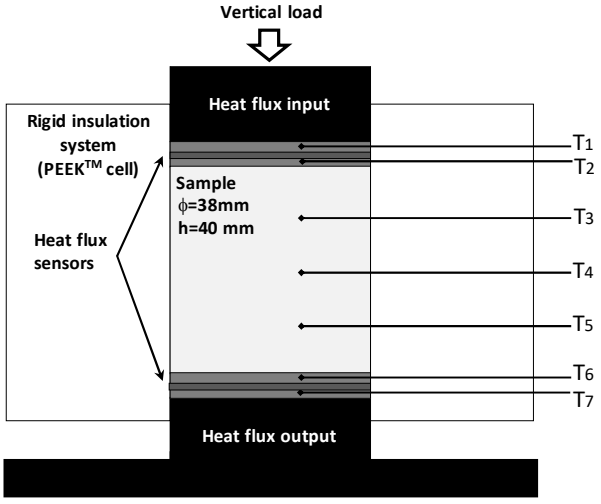

Fig. 1. Thermal conductivity cell with 7 thermocouples Ti.

3 Results and interpretation

Figures 2 and 3 display the time evolutions of temperatures recorded during one of the tests and its inflow and outflow determined using Equation (1). The steady-state conditions were approximately reached after 260 min. The thermal conductivity was not homogenous along the sample height (internal thermocouples T_3, T_4 and T_5), as observed by [15]. Different phenomena largely associated with local soil volume and water content heterogeneities as well as their changes through the thermal test itself (final water

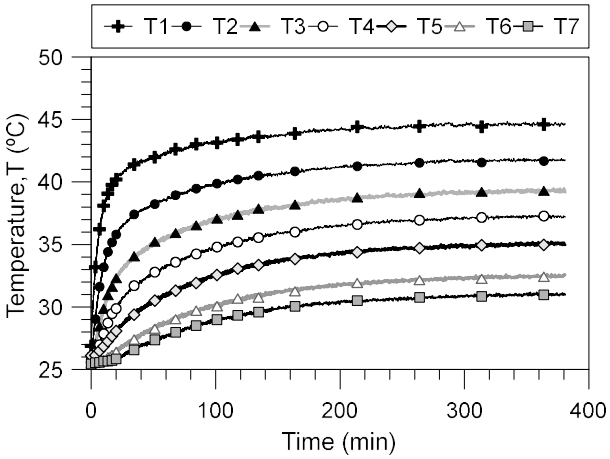

Fig. 2. Evolution of temperatures of a thermal conductivity test (sample Comp-OPA-2).

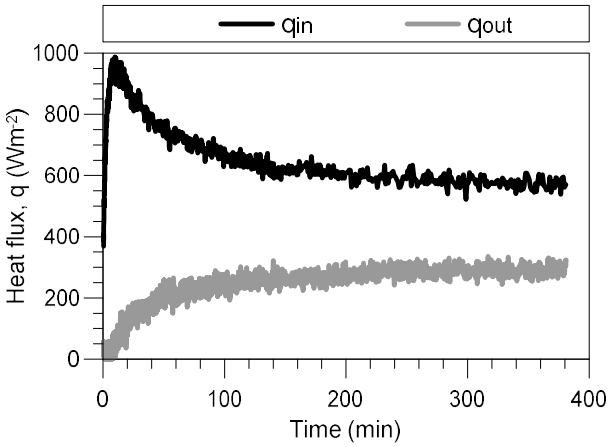

Fig. 3. Time evolution of inflow and outflow heat fluxes of a thermal conductivity test (sample Comp-OPA-2).

contents are slightly lower close to the top cap at the higher temperature) lead to temperature differences between equidistant internal points in the soil sample. Nevertheless, the compaction methodology allowed for obtaining relatively homogeneous samples; thus, the temperature differences were small.

Under steady-state conditions, the global thermal conductivity λ was computed using Fourier's law:

$$\lambda = q_{ave}\, L/\Delta T \quad (2)$$

where q_{ave} represents the average inflow and outflow heat fluxes, L the sample height and ΔT the difference between thermocouples T_2 and T_6.

Figure 4 displays the thermal conductivity results versus the degree of saturation before the thermal tests. Two phenomena are perceived, the influence of the initial degree of saturation in compacted OPA samples and anisotropic features in intact OPA samples. The data indicate the reduction in thermal conductivity with decreasing initial degree of saturation on compacted samples. Regarding anisotropic features, thermal conductivity determined with heat flow parallel to beddings planes $\lambda \parallel$ is higher than the one with heat flow orthogonal to bedding planes λL. The fact is consistent with the observations made by other authors in Opalinus

Clay (see Table 3) and in other bedded clay formations such as Boom Clay [16–19], Ypresian clays [14,15] and Callovo-Oxfordian claystone [18,20,21]. Figure 4 also plots the fitting curve that describes the trend of thermal conductivity with the degree of saturation in compacted samples (solid line). This fitting follows the geometric mean model [22] with:

$$\lambda = \lambda_{sat}^{Sr} \lambda_{dry}^{(1-Sr)} \; ; \; \lambda_{sat} = \lambda_s^{(1-n)} \lambda_w^{n} \; ; \; \lambda_{dry} = \lambda_s^{(1-n)} \lambda_a^{n} \qquad (3)$$

where the subscripts 'sat', 'dry', 's', 'w' and 'a' stand for saturated, dry, solid, water and air, respectively, n is the porosity (n = 0.253), and S_r is the degree of saturation.

Figure 4 also presents the evolution of the sample OPA-bed‖ (dashed lines) following the same variation with the degree of saturation. Thereby, the value of $\lambda\|$ at fully saturated conditions would be around 3.0 $Wm^{-1}K^{-1}$. The anisotropy ratio in terms of thermal conductivity (η_T = 1.87*)* is determined using the values of $\lambda\|$ and $\lambda\perp$ at S_r=1 as (refer to Table 3):

$$\eta_T = \lambda\| / \lambda\perp \qquad (4)$$

4 Discussion and conclusions

Table 3 summarises the thermal conductivity values (at two different orientations) and the anisotropy ratio of intact OPA in the present study and state-of-the-art results. This last group of results is obtained from studies focused on investigating the thermal properties and thermo-hydro-mechanical behaviour of Opalinus Clay in the framework of a deep geological repository of radioactive waste (references are reported in the table). These studies were based on data extracted from in situ tests (HE-B, HE-C, HE-D, HE-E and FE experiments) at the Mont Terri Underground Research Laboratory (URL, the overburden height varies between 250 and 320 m) or from samples retrieved from shaly

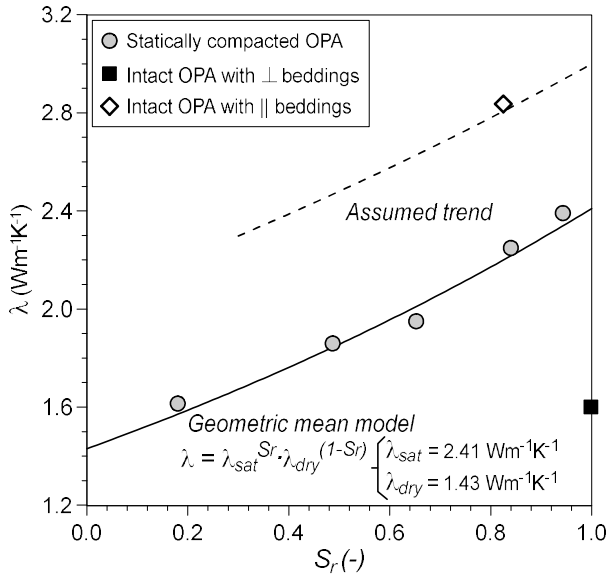

Fig. 4. Thermal conductivity measurements of compacted and intact samples for two different orientations (heat flux orthogonal and parallel to bedding planes) versus the degree of saturation.

Table 3. Summary of thermal conductivity data of intact Opalinus Clay. Modified from [14].

Source	$\lambda\perp$ ($Wm^{-1}K^{-1}$)	$\lambda\|\|$ ($Wm^{-1}K^{-1}$)	η_T (-)
Present study[1] (shaly facies, 300-340 m depth)	1.60 (Sr = 99.8%)	2.83 (Sr = 82.5%) 3.01* (Sr = 100%)	1.87
[23] [1] (shaly facies, 622 and 642 m depth)	1.79 and 1.26	3.23 and 2.04	1.80 and 1.62
[24] [3] (HE-C)	0.55 and 1.07	1.84 and 1.90	3.34 and 1.78
[25] [3] (HE-D)	1.20	2.10	1.75
[26] [2] (shaly facies, URL depth)	-	2.50	-
[27] [3] (HE-B, HE-D, HE-E)	1.20	2.15	1.80
[28] [3] (FE)	1.30	2.40	1.84

[1] direct measurement on samples at the laboratory
[2] backanalysed from laboratory heating tests
[3] backanalysed from in situ heating tests at the URL
* Value assumed at fully saturated conditions

facies at different depths. Different methodologies were employed to determine the thermal conductivity gathered in Table 3: direct measurements on samples at the laboratory (superscript [1]), backanalysed from laboratory tests (superscript [2]) and backanalysed from in situ heating tests at the URL (superscript [3]). Both laboratory measurements and backanalyses are not free of drawbacks. The lab measurements in Opalinus Clay [23] were performed with a divided bar apparatus under high confining stress, obtaining values comparable to the backanalysed ones. Regarding the backanalysed values, in general, there is a good agreement; just the values reported by [24] differ. These lower values were related to the presence of an intensive fractured zone or a bed of carbonated rock with less quartz content (the HE-C experiment was close to the calcareous sandy facies).

The values determined in this study are slightly higher, but the anisotropy ratio is comparable with the state-of-the-art data. The differences result from slight changes in mineralogical composition and porosity. Mineralogical composition, porosity and degree of saturation strongly affect the thermal conductivity of geomaterials.

Regarding the thermal conductivity of artificially prepared samples, their mineralogy is the same as the intact OPA-bed‖ since the dry powder soil belongs to the same core. The differences in the values of intact samples are mainly associated with the soil microstructure (arrangement of grains and pore network). The value of the compacted sample lies close to the mean value of $\lambda\|$ and $\lambda\perp$. Despite the different microstructure generated by compaction at different hydraulic states compared to the natural damaged state,

the study allows determining the consistent effects of degree of saturation on the thermal conductivity, which has a crucial role on the material during tunnel ventilation and their associated RH variations.

Nevertheless, as observed in Figure 4, the values graphically fitted for thermal conductivity at saturated and dry conditions were 2.41 and 1.43 $Wm^{-1}K^{-1}$, respectively. These values did not agree with $\lambda_{sat} = 2.26\ Wm^{-1}K^{-1}$ and $\lambda_{dry} = 1.02\ Wm^{-1}K^{-1}$ using Equation (3) and the reference values of λ_w (0.598 $Wm^{-1}K^{-1}$ at 20°C), λ_a (0.026 $Wm^{-1}K^{-1}$ at 20°C), and $\lambda_s = 3.55\ Wm^{-1}K^{-1}$, which was estimated using the simplified version of the geometric mean method proposed by [29] for materials with quartz content $q < 0.20$:

$$\lambda_s = 7.7^{q} \cdot 3.0^{(1-q)} \quad (5)$$

The temperature dependence of thermal conductivity can not justify the fitted values of λ_{sat} and λ_{dry}. The reference value of λ_w increases by 6% (0.634 $Wm^{-1}K^{-1}$) at the average temperature of the tests (40°C). By contrast, the dependence in λ_s and λ_a is negligible in this temperature range. Likewise, the changes in S_r and n because of the thermal expansion of the constituents and the irreversible thermal strains were minimal.

A larger value of $\lambda_s = 3.78\ Wm^{-1}K^{-1}$ can also explain the fitted value $\lambda_{sat} = 2.41\ Wm^{-1}K^{-1}$. Nevertheless, it does not justify λ_{dry}. It may also be assumed that the thermal conductivity of the liquid phase is a combination of adsorbed/ice-like water (λ_{w_ad} = 2-3 $Wm^{-1}K^{-1}$, according to [30]) and free water, given the mineralogical properties of OPA. To reach the fitted value of λ_{sat}, the thermal conductivity of the liquid phase would be 0.78 $Wm^{-1}K^{-1}$, which agrees with the value reported by [15] when studying the impact of S_r in artificially prepared samples of Ypresian clays. On the other hand, the presence of adsorbed water still bonded to clay particles after oven-drying at 105ºC also affect the value of λ_{dry}, increasing its theoretical value.

Figure 5 plots the thermal conductivity values of the compacted OPA samples ($\rho_d = 2.0\ Mg/m^3$) together with experimental values measured by different authors on fine-grained clayey materials. A clear influence of the degree of saturation and dry density can be observed. Those results reported by [15,31] were measured with the same testing equipment used in this study and under confined conditions. Their samples had different mineralogical compositions but were statically compacted at the same dry density (1.6 Mg/m^3). They aimed to evaluate the impact of the clay mineralogy, quartz content and degree of saturation. Samples with higher quartz and smectite contents (Core-022a-mod-Qz-31%) showed higher thermal conductivity than the denser OPA samples. The values reported by [32] were measured with the needle probe under unconfined conditions on samples with different mineralogy compacted at $\rho_d = 1.5\ Mg/m^3$.

In summary, this study's results have revealed that the maximum variation of thermal conductivity at the usual range of the degree of saturation encountered in tunnels (S_r≈70-100%) corresponds to around 0.5 $Wm^{-1}K^{-1}$.

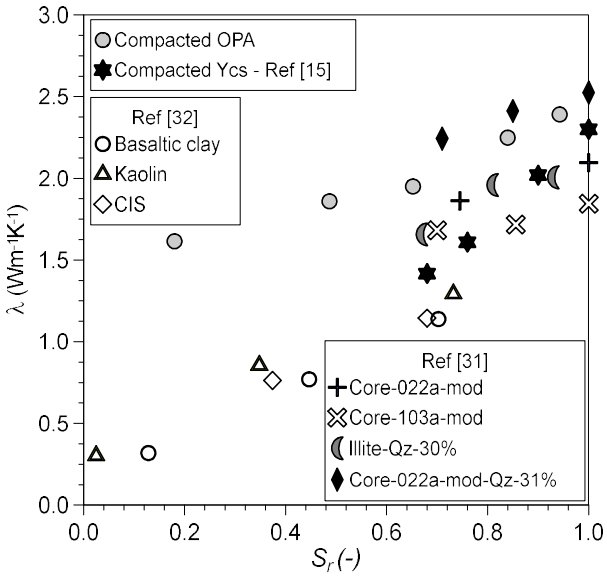

Fig. 5. State-of-the-art thermal conductivities of unsaturated fine-grained clayey materials.

We would like to gratefully acknowledge the financial support by the German Research Foundation (DFG) through the collaborative research centre (SFB 837) subproject A5 and Dr Martin Ziegler (Department of Earth Sciences, ETH Zurich) for providing the samples. The drilling and sampling works were financed by the Swiss Federal Nuclear Safety Inspectorate (ENSI) in the frame of the STB (Sanierungstunnel Belchen) project.

References

1. H. H. Einstein, Tunelling Undergr. Sp. Technol. **15**, 49 (2000).
2. C. Amstad, K. Kovári, *Untertagebau in Quellfähigem Fels. Research Report 52/94, 5408.01* (2001).
3. W. Steiner, P. K. Kaiser, G. Spaun, Geomech. Tunn. **4**, 141 (2011).
4. A. Ramon, E. E. Alonso, S. Olivella, Geotechnique **67**, 968 (2017).
5. E. Alonso, A. Ramon-Tarragona, L. Verda, Rock Mech. Rock Eng. (2022).
6. M. Ziegler, A. Alimardani Lavasan, S. Loew, Tunn. Undergr. Sp. Technol. **128**, 104649 (2022).
7. A. Ferrari, V. Favero, P. Marschall, L. Laloui, Int. J. Rock Mech. Min. Sci. **72**, 61 (2014).
8. A. Minardi, E. Crisci, A. Ferrari, L. Laloui, Geotech. Lett. **6**, 144 (2016).
9. V. Favero, A. Ferrari, L. Laloui, Eng. Geol. **208**, 128 (2016).
10. E. Crisci, A. Ferrari, S. B. Giger, L. Laloui, Eng. Geol. **251**, 214 (2019).
11. M. Ziegler, S. Loew, *Investigations in the New TBM-Excavated Belchen Highway Tunnel - Program, Design and Installations (Part 1): ENSI*

Research and Experience 2016. (ENSI-AN-9961) (2017).

12. M. Ziegler, B. Brixel, A. Alimardani Lavasan, F. Christ, *Investigations in the New TBM-Excavated Belchen Highway Tunnel : Summary and Conclusions. ENSI Research and Experience 2021. (ENSI-AN-11284)* (2022).
13. R. Cardoso, E. Romero, A. Lima, A. Ferrari, in *Proc. 2nd Int. Conf. Mech. Unsaturated Soils*, edited by T. Schanz (Springer Proceeding in Physics, Weimar, Germany, 2007), pp. 79–93.
14. N. Sau, Thermo-Hydro-Mechanical Behaviour of a Deep Argillaceous Formation, Universitat Politècnica de Catalunya, 2021.
15. E. Romero, N. Sau, A. Lima, H. Van Baelen, X. Sillen, X. Li, Geomech. Energy Environ. **8**, 62 (2016).
16. R. Charlier, S. Chalandar, F. Collin, A. Dizier, *Deliverable D13 –Annex 4. In Situ Heating Test ATLAS in Mol. TIMODAZ Project, F16W-CT-2007-036449* (2010).
17. G. J. Chen, X. L. Li, Proc. 2nd Int. Symp. Comput. Geomech. (COMGEO II) 640 (2011).
18. B. Garitte, A. Gens, J. Vaunat, G. Armand, Rock Mech. Rock Eng. **47**, 111 (2014).
19. L. Q. Dao, Y. J. Cui, A. M. Tang, J. M. Pereira, X. L. Li, X. Sillen, Eng. Geol. **195**, 196 (2015).
20. N. Conil, B. Gatimiri, G. Armand, *Premiers Résultats de l'expérimentation TED. ANDRA Report D.RP.AMFS.10.0067* (2010).
21. M. Jobmann, S. Li, M. Polster, M. Breustedt, R. Schlegel, P. Vymlatil, J. Willet, J. Geol. Resour. Eng. **3**, 125 (2016).
22. O. T. Farouki, *Thermal Properties of Soils. CRREL Monograph 81-1* (1981).
23. Nagra, *Sondierbohrung Benken: Untersuchungsbericht* (2001).
24. C. Mügler, M. Filippi, P. Montarnal, J. M. Martinez, Y. Wileveau, J. Appl. Geophys. **58**, 112 (2006).
25. Y. Wileveau, T. Rothfuchs, *THM Behaviour of Host Rock (HE-D Experiment). Study of Thermal Effects on Opalinus Clay. Synthesis Report. Mont Terri Technical Report TR 2006-01* (2007).
26. J. J. Muñoz, E. E. Alonso, A. Lloret, Géotechnique **59**, 293 (2009).
27. A. Gens, K. Wieczorek, I. Gaus, B. Garitte, J. C. Mayor, K. Schuster, G. Armand, J. L. García-Siñeriz, T. Trick, Swiss J. Geosci. **110**, 269 (2017).
28. A. Alcolea, P. Marschall, F. Team, *FE-Modelling Task Force / Task 1: Validation of Thermally Induced THM Effects in the Rock around the FE-Tunnel. NAGRA Arbeitsbericht NAB 19-040* (2019).
29. O. Johansen, Thermal Conductivity of Soils, Norwegian University of Science and Technology, , Trondheim, 1975.
30. J. Cheh, Y. Gao, C. Wang, H. Zhao, H. Fang, J. Stat. Mech. Theory Exp. **2013**, P06009 (2013).
31. M. F. Ballesteros, Thermal Properties in Artificially Prepared Samples Mimicking Deep Ypresian Clays. MSc Thesis, Universitat Politècnica de Catalunya, 2020.
32. D. Barry-Macaulay, An Investigation on the Thermal and Thermo - Mechanical Behaviour of Soils, Monash University, 2013.